Low temperature Topographically Selective Deposition by Plasma Enhanced Atomic Layer Deposition with ion bombardment assistance

Taguhi Yeghoyan, Vincent Pesce, Moustapha Jaffal, Gauthier Lefevre, Rémy Gassilloud, Nicolas Posseme, Marceline Bonvalot, Christophe Vallée

Low temperature Topographically Selective Deposition by Plasma Enhanced Atomic Layer Deposition with ion bombardment assistance

Taguhi Yeghoyan,[1,a)] Vincent Pesce,[1] Moustapha Jaffal,[1] Gauthier Lefevre,[1] Rémy Gassilloud,[2] Nicolas Posseme,[2] Marceline Bonvalot,[1,3] and Christophe Vallée[1,4]

[1]University Grenoble Alpes, CNRS, CEA/LETI-Minatec, Grenoble INP, LTM, F-38054 Grenoble, France [2]CEA-LETI, Minatec Campus, F-38054 Grenoble, France

[3]University of Tsukuba, Tsukuba 305–8573, Japan

[4]SUNY POLY, CNSE, Albany, New York 12203, USA

Area selective deposition via atomic layer deposition (ALD) has proven its utility in elementary nanopatterning processes. In the case of complex 3D patterned substrates, selective deposition processes lead to vertical sidewall coverage only, or top and bottom horizontal surface coverage only, to enable advanced nanopatterning and further miniaturization of microelectronic devices. While many fabrication strategies for vertical only Topographically Selective Deposition (TSD) have already been developed, the horizontal TSD case needs further attention. In this work, we propose a versatile route for the TSD on 3D top and bottom horizontal surfaces along with a proof-of-concept for such selective Ta_2O_5 thin film deposition. The strategy at stake relies on a plasma enhanced atomic layer deposition process assisted by energetic ion bombardment during the plasma step and followed by a postgrowth wet etching step. The effectiveness of this strategy is based on a careful adjustment of processing temperatures purposely set at low temperature, most probably below the ALD temperature window. Anisotropic ion bombardment via substrate biasing during the plasma step provides an extra amount of thermal energy only to exposed horizontal surfaces, which in turn enables a selective densification of the thin film under growth. The difference in thin film density on horizontal and vertical surfaces enables the property-selective etching of vertical surfaces, generating horizontal TSD. A proof-of-concept for such low temperature TSD is shown in the case of 3D trenched substrates with an aspect ratio of 14.

I. INTRODUCTION

A. Introduction to area selective deposition

Area Selective Deposition (ASD) by Atomic Layer Deposition (ALD) is gaining increased attention as a strategy for bottom-up thin film deposition that can potentially avoid technically challenging multipatterning lithography steps for the production of advanced nano- and microelectronic devices. In this regard, ASD is particularly attractive for high throughput manufacturing of nanoelectronic components with 3D architectures such as 3D solid-state batteries,[1] 3D photonic devices,[2] as well as microelectronic logic and transistor devices.[3–5] Considering 3D architectures such as trenches or pillars, two distinct objectives can be identified for Topographically Selective Deposition (TSD). The first objective is to produce a thin film on vertical surfaces only, e.g., for potential applications such as spacers for nanopatterning, liners, or diffusion barriers.[4,6–8] The second objective is to produce a thin film on horizontal (top and/or bottom) surfaces only, for applications such as nanowire coating,[9] self-aligned gates and contacts,[4] trench filling, hard mask deposition,[10] or edge placement error correction.[11] Numerous strategies have already been proposed in the literature for TSD of 3D substrates. For instance, deposition on vertical 3D trench sidewalls can be achieved by surface deactivation by *in situ* fluorocarbon deposition before growth[12] or by

ex situ self-assembled monolayers grafting.[13] 3D vertical TSD can also be achieved thanks to an *in situ* Atomic Layer Etching (ALE)-like anisotropic etching step after conformal deposition[14] or by a supercycle approach based on alternating deposition and etching steps during thin film growth.[9]

Another TSD strategy has recently emerged, which is based on a standard plasma enhanced atomic layer deposition (PEALD) process combined with an additional substrate RF polarization during each plasma step and followed by a postdeposition wet etching step. This substrate polarization induces a directional ion flux impinging perpendicularly to the substrate, and it in turn alters the physical properties and hence the Wet Etch Rate (WER) of the thin film under growth. Depending on ion energies, the deposited material, and the precursor chemistry, this ionic bombardment assistance can either improve or degrade the physical properties of the film, and only horizontal surfaces are concerned when dealing with 3D substrates. Hence, by carefully tuning the average kinetic energy of impinging ions, the thin film properties on exposed horizontal surfaces are modified and can later be maintained or removed during a subsequent postgrowth wet etch. Thus, a selectively deposited film only on either horizontal or vertical surfaces of the 3D substrate can be obtained.[8,15]

In this study, we develop a TSD strategy by using ion bombardment in a nonideal PEALD regime, i.e., below the well-known processing ALD temperature window. When the temperature of the process is intentionally set below or above such an ALD window, the GPC (Growth Per Cycle) and/or density of the material are strongly modified. Ionic bombardment assistance during PEALD provides an additional control knob among growth parameters, analogous to a temperature modulation that allows restoring the surface dependent growth regime of the ALD window. This is attributed to the overall increase in thermal energy (ionic bombardment + temperature) at the surface of the film under growth. Consequently, surface reactions can be activated by ion bombardment, such as adatom diffusion, creation of active sites, or desorption of adsorbed species.[16] Therefore, when the ion flux is intentionally directed perpendicular to the surface, the thin film properties will then be altered only on exposed surfaces of 3D patterns, potentially inducing a difference in the growth regime on surfaces normal and parallel to the ion flux, respectively. In the following, this strategy is first described, and an experimental proof-of-concept is then given. As mentioned above, this work relies on a standard PEALD process carried out with a basic ALD recipe but at a processing temperature deliberately set much lower than that recommended for the metallic precursor at stake. This generates a poor-quality deposit with a high level of impurities and a low density, while the conformal aspect of ALD is preserved. Then, an anisotropic ion bombardment step, using a medium ion energy, is inserted within the process, which provides the extra thermal activation required to improve the density and purity on surfaces exposed to the ion flux (namely, horizontal top and bottom surfaces). The difference in material properties on vertical and horizontal surfaces is expected to induce a WER difference enabling TSD.

B. TSD at low temperatures: Basic principles

1. Material growth regimes in ALD

The thermal or plasma-based ALD process with temperature is illustrated in Fig. 1. In this schematic, four different material growth regimes, besides the ALD plateau regime, are generally identified.[17,18] At lower temperatures, incomplete reaction (regime A) or condensation (regime B) can happen, both resulting in a low material density. Regime A leads to an increasing GPC with temperature due to a limited precursor adsorption,[19–21] whereas regime B leads to a decrease in the GPC when the temperature increases due to precursor molecule condensation, which results in organic ligand incorporation into the deposited materials.[22–24] At temperatures above the ALD window, precursor decomposition (regime C) or adatom desorption (regime D) can take place. Regime C indicates the onset of the chemical vapor deposition growth mode, evidenced by an increasing GPC with temperature, due to precursor thermal decomposition at the substrate surface. Finally, in regime D, the GPC decreases with temperature because of enhanced desorption of adsorbed precursor molecules. It should also be mentioned that the ALD plateau itself can be nonideal, especially when metal-organic precursors are used. This is evidenced by a small GPC decrease when the temperature is increased (indicated by the dashed line in Fig. 1).[17,19,24–26]

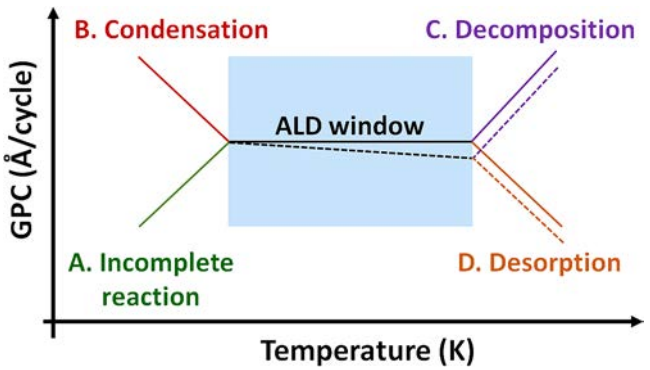

FIG. 1. Schematic GPC temperature behavior defining the ALD temperature window, as described in Refs. 18 and 27.

2. Ion bombardment assistance during PEALD

It is generally accepted that PEALD extends the thermal ALD temperature window of a given precursor toward the lower temperature region because the lower thermal energy of the process is compensated by exposure to highly reactive plasma species, such as radicals, ions, and photons.[27,28] At lower deposition temperatures, the physical properties of PEALD thin films can be further modulated by adjusting the duration of the plasma step, i.e., the ion dose on the thin film under growth. However, an interesting alternative for this purpose is to apply an additional waveform RF bias voltage to the substrate during the plasma step itself.[8] The resulting time-averaged bias voltage V_{DC} enables extraction of positively charged reactive plasma species with a tunable incident kinetic energy. This ion flux is then accelerated through the plasma sheath in a perpendicular trajectory to the substrate.[29] The impact of such an ionic bombardment during the second half-reaction of the PEALD process depends on the ionic species at stake and on their incident kinetic energy.[16] At medium ionic energy, typically from 30 to

150 eV, surface reactions such as enhanced combustion and adatom diffusion are favored, boosting thin film growth. Consequently, the first half-reaction of the following PEALD cycle is also activated thanks to improved ligand exchange mechanisms and activation of nucleation sites after the plasma step.[23,30] On the other hand, at high incident ionic energy (*larger than* 150 eV), phenomena such as sputtering, roughening, and/or implantation can prevail with detrimental effects on the physical properties of PEALD thin films.[16]

3. Investigated top and bottom TSD strategy: Top and bottom deposition by density modification in the low temperature regime

Performing a standard ALD process at low temperature, which is expected to be outside of the ALD plateau, can result in a nonoptimized thin film density. As an example, in the condensation regime B, ligands from the metal-organic precursor can be incorporated in the solid film, leading to light contaminants such as [C] or [H], as well as nonstoichiometric [O] or [N] contents, in the case of oxide or nitride deposition. This can result in a lower density of the deposited material. In such a case, ion bombardment assistance can be used to improve the properties of the deposited thin film on top and bottom surfaces, as illustrated in Fig. 2. In this figure, a deposition carried out at a temperature below the ALD window (regime A or B) can result in a low material density due to ligand incorporation. Energetic ions added to the process induce enhanced ligand removal during the plasma step, thus decreasing contamination in the material and, consequently, increasing its density. Hence, when deposition is carried out in 3D structures, horizontal surfaces exposed to the ion flux could exhibit a larger density as compared to vertical surfaces. Finally, a postdeposition selective etching step (wet or dry) can lead to top and bottom selective deposition, thanks to the higher etching rate of the lower density material.

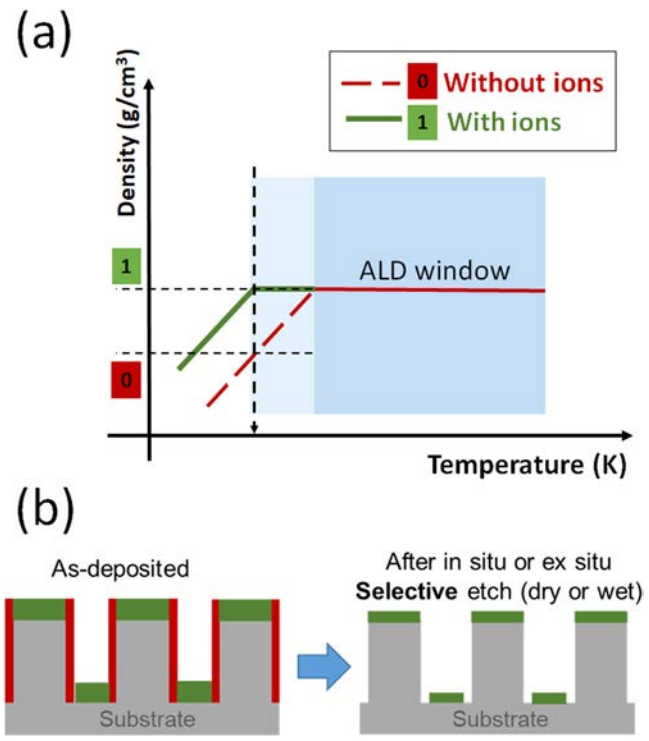

FIG. 2. (a) Schematic illustrating the impact of ion bombardment on the thin film density for a process carried out below the ALD temperature window and (b) subsequent TSD strategy in 3D structures.

In this paper, we focus on such selective deposition strategy based on low processing temperatures and combined with an anisotropic ion bombardment during the PEALD process. The proof-of-concept of this low temperature TSD approach is carried out for Ta_2O_5 thin film deposition. Ta_2O_5 is chosen since it is often used in semiconductor manufacturing, for example, for antireflective coatings or electrical isolation. For given application examples, it is necessary that the deposited film exhibits high refractive index and high density. In addition, as of general trend in semiconductor manufacturing, it is desirable that thin films can be deposited at very low temperatures with a reasonable growth rate. If the prediction given above is correct, Ta_2O_5 thin film density is expected to improve on surfaces exposed to the ion flux and a postgrowth isotropic wet etching step is, thus, expected to selectively remove coating on vertical sidewalls.

II. EXPERIMENT

Ta_2O_5 thin films are deposited in a remote-plasma, low-pressure, hot-wall commercial ALD reactor (FlexAl, Oxford Instruments) with an inductively coupled plasma (ICP) RF source operating at a frequency of 13.56 MHz. The substrate is additionally biased with a similar matching box (13.56 MHz) operating at a tunable incident RF power of up to 80 W corresponding to a time-averaged substrate bias voltage V_{DC} of up to −315 V.

The first PEALD half-reaction of Ta_2O_5 involves the t-butylimino-tris(dimethylamino)tantalum (TBTDMT) (99.99% purity) metal-organic precursor diluted in 100 SCCM Ar flux. This step lasts for 1.5 s at a chamber pressure of 80 mTorr and is followed by a 3 s purge step. The second half-reaction consists of a 2 s, 60 SCCM O_2 gas stabilization at a chamber pressure of 15 mTorr, after which the plasma is ignited for 2 s with a power of 300 W to the ICP unit. When needed, the substrate is biased during the whole plasma step. This is then followed by a 2 s purge with a 100 SCCM Ar flux at a chamber pressure of 80 mTorr.

Depositions are first performed on planar Si substrates with a 1.5 nm native SiO_2 for Ta_2O_5 material property characterization. Two experimental parameters, namely, substrate stage temperature and substrate bias power, have been varied from 100 to 400 °C and 0–80 W (V_{DC} = 0 to −315 V), respectively. Then, the deposition has been carried out in 3D structures with applied substrate bias and followed by a postgrowth wet etch in 5% hydrofluoric acid (HF) to lead to TSD. The 3D structures are fabricated by deep reactive ion etch according to a Bosch process alternating octafluorocyclobutane (C_4F_8) passivation and hexafluoride (SF_6) etching steps.

The film thickness is controlled by an *in situ* Film sense FS-1 multiwavelength ellipsometer working in the visible range and confirmed by *ex situ* spectroscopic ellipsometry (SE) (Horiba Scientific, AutoSE), scanning electron microscopy (SEM, Zeiss Merlin), and x-ray reflectometry (XRR, PANalytical X'pert PRO). *Ex situ* SE with a Tauc–Lorentz dielectric function model is used to estimate the thickness and refractive index values. Density and thickness measurements are extracted by XRR with a general algorithm calculation using JVXRR software.

III. RESULTS AND DISCUSSION

A. Proof-of-concept of top and bottom TSD on 2D planar substrates

Ta_2O_5 films with a thickness of ~10 nm were used to investigate the PEALD temperature window as a function of substrate stage temperature. The obtained GPC, material density, and refractive index of thin films prepared without any applied bias voltage are presented in Fig. 3. Looking at the results, it is rather evident that the ALD plateau is nonideal. Nevertheless, combining both GPC and material properties results, we can deduce that low temperature growth can be assigned to the condensation regime (regime B) with higher GPC and lower density and refractive index, in agreement with conventional ALD regimes.[24] Such a nonideal ALD plateau has already been reported for Ta_2O_5 thin films deposited from TBTDMT and derivatives, both by thermal[23,25,31,32] and PEALD processes,[24,33,34] and has been attributed to temperature-activated ligand exchange reactions during the first half-ALD-reaction[23,35] and combustion

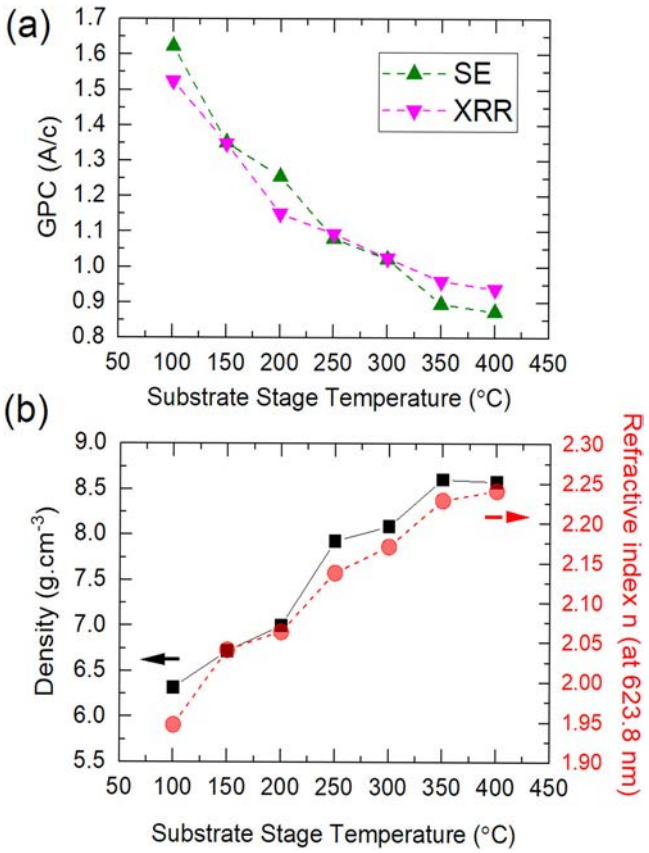

FIG. 3. Nonideal ALD window of an ~10 nm thick Ta_2O_5 PEALD thin film with no applied bias voltage: (a) growth per cycle and (b) material density and refractive index as a function of substrate stage temperature. The dashed lines represent a visual guide.

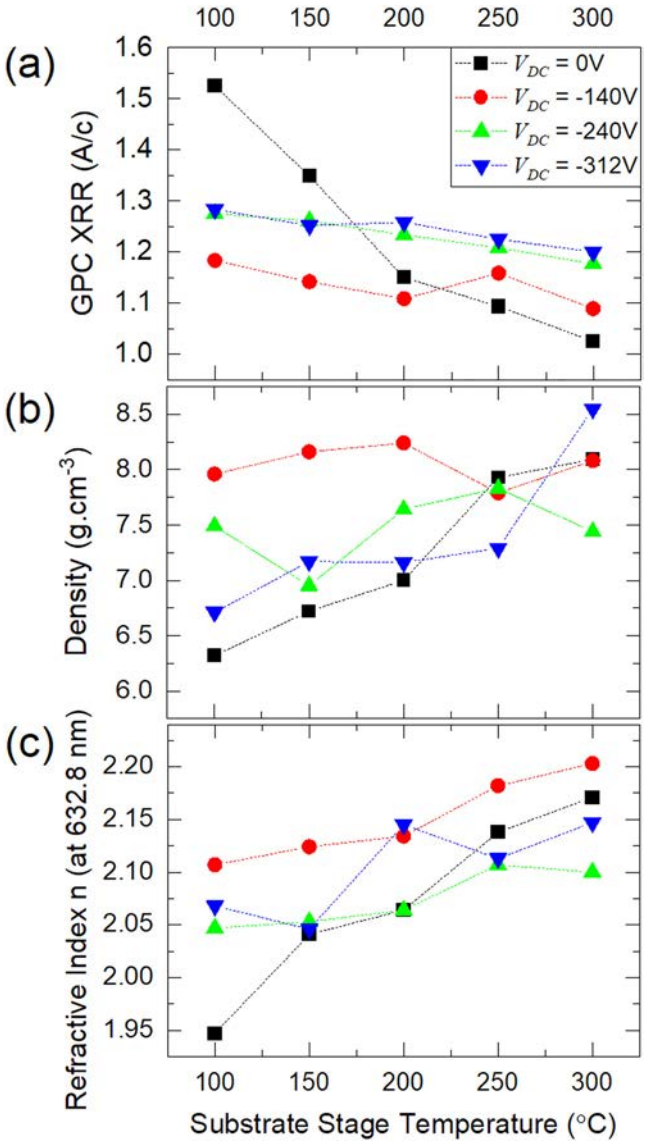

FIG. 4. Nonideal ALD window of Ta_2O_5 PEALD as a function of substrate stage temperature for various time-averaged substrate bias voltages V_{DC}: (a) growth per cycle, (b) material density, and (c) refractive index. The dashed lines represent a visual guide.

reactions by oxidizing agents during the second half-reaction.[30,33,35] Hence, at low deposition temperature, an incorporation of *tert*-butyl ligands leading to a low density porous Ta_2O_5 deposit.

In a previous paper,[16] we have already discussed in detail the extent to which PEALD thin film physical properties can be significantly improved by exposing the thin film at stake to energetic ionic bombardment during the second half-cycle of the PEALD process. Figure 4 shows the impact of substrate bias on the GPC, thin film density, and refractive index for temperatures ranging from 100 to 300 °C. It can be observed that substrate biasing significantly mitigates the GPC decrease with temperature with the strongest effect at $V_{DC} = -140$ V. Using such low ion energy bombardment, the GPC becomes rather flat throughout all deposition temperatures used, ranging between 1.1 and 1.2 A/c. Moreover, material properties are greatly enhanced even for deposition at 100 °C, having values close to stoichiometric, bulk Ta_2O_5 ($n = 2.16$ and 8.2 g/cm^3). Such encouraging results can be attributed to the ion bombardment energy, which favors TBTDMT amine bond breaking and organic ligand combustion, as confirmed by improved density and refractive index of the thin film. On the other hand, at temperatures above 200 °C, no clear trend can be deduced in the GPC behavior, and a quantitative analysis of modified material properties seems hazardous. A deep investigation of involved mechanisms, such as implantation and sputtering, has already been reported[8] and is out of scope of the present work.

However, the important point to underline here is that medium energy substrate biasing strongly improves material properties at deposition temperatures ≃100 °C.

The density improvement for deposition at 100 °C is further confirmed from XRR data (Fig. 5), which shows that the XRR critical angle is shifted toward higher incident angles for medium ion energy, indicating a higher film density. Moreover, Fig. 5 also shows an improved oscillatory pattern at higher angles, indicating that surface roughness decreases with increasing ion bombardment energy. This, along with the decay rate of oscillations at higher angles, indicates an interfacial roughness decrease at $V_{DC} = -240$ V and is consistent with sputtering phenomena. Finally, a lower

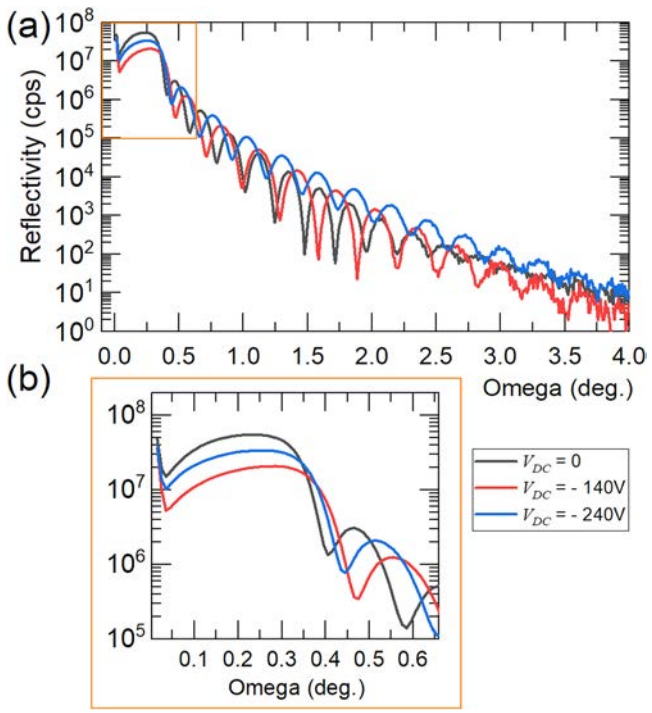

FIG. 5. XRR measurements of an ~10 nm Ta_2O_5 PEALD deposited at 100 °C as a function of time-averaged substrate bias voltage V_{DC}: (a) full scan and (b) zoom on the critical angle region.

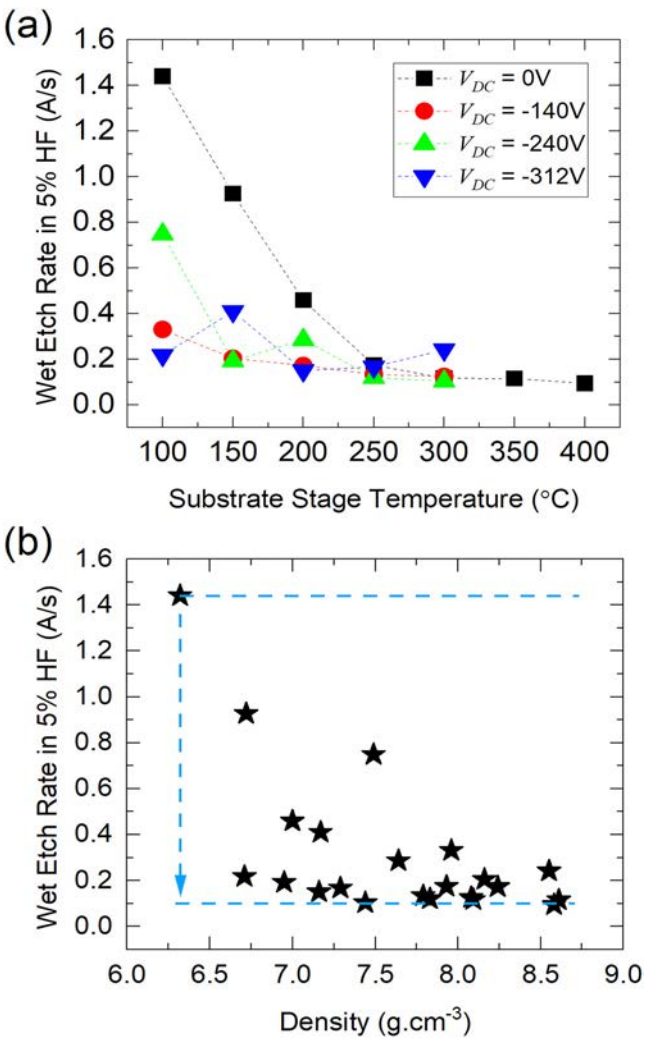

FIG. 6. WER of Ta_2O_5 thin films deposited by PEALD at 100 °C and etched in 5% HF as a function of (a) substrate stage temperature and (b) Ta_2O_5 thin film density. The dashed lines represent a visual guide.

oscillation frequency is also consistent with a GPC decrease upon increasing ionic bombardment energy.

The benefits induced by ion bombardment on PEALD material density can also be evidenced from WER measurements in 5% HF (Fig. 6). As expected, the WER is inversely proportional to the deposition temperature when no substrate bias is applied. However, a significant decrease in the WER can be observed when a substrate bias is applied, especially at T ≈ 100 °C in agreement with improved thin film density under ion bombardment [Fig. 6(a)]. Figure 6(b) further confirms that the WER decreases with thin film density, regardless of growth conditions (T, V_{DC}).

B. Proof-of-concept of top and bottom TSD on 3D substrates

The proof-of-concept for low temperature TSD elaboration is performed with PEALD process parameters leading to the largest change in thin film density under applied substrate bias as compared to the no-bias density value. This corresponds to $V_{DC} = -140$ V at 100 °C. Due to the directionality of the ion flux perpendicular to the substrate, the thin film deposited on horizontal surfaces is expected to exhibit physical properties (density and WER) similar to that of Ta_2O_5 thin films grown under −140 V applied bias, whereas 3D sidewall coatings should

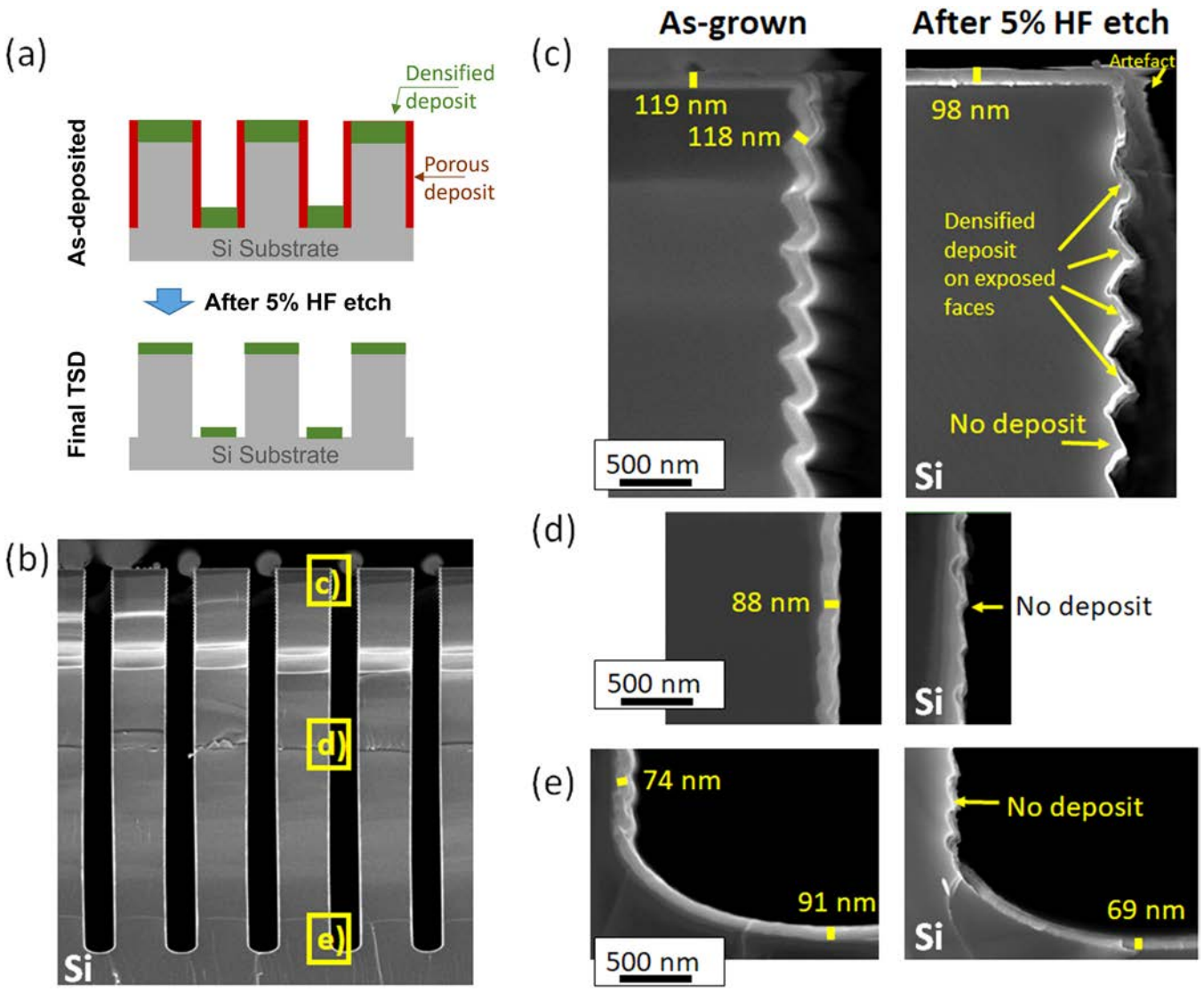

FIG. 7. (a) Fabrication schematic of bottom and top only deposits by ion bombardment assisted PEALD followed by a wet etching step in 5% HF. (b) SEM image of 3D trenches with AR = 14. (c)–(e) Detailed SEM images of ∼100 nm Ta_2O_5 thin film: as grown (left) and after postgrowth wet etching (right) in the top, middle, and bottom regions of the 3D trench. Note the densified thin film on exposed surfaces of the scalloping pattern [(c), right].

lead to a low Ta_2O_5 density and a large WER, similar to that of a thin film grown without any applied substrate bias. Figure 7 shows the TSD fabrication sequence for both as grown- and HF-etched 3D trenches. SEM images of the top, mid-height of sidewall, and bottom regions of the 3D trench are also shown in Figs. 7(c)–7(e), respectively. It can be observed that only top and bottom deposits are present after HF etching, although their thickness has decreased by a factor of 18% and 24%, respectively, as compared to as-grown thicknesses. Top-versus-bottom conformity is also observed to level off after etching. These two observations can be taken as an indication that the ion flux and incident ion kinetic energy are gradually lost within the depth of the 3D trench, which most likely results in lower thickness and density of the thin film in the bottom mesas. Moreover, no deposit is observed on sidewalls of the 3D trench, thus confirming a successful TSD fabrication methodology. Interestingly, the scalloping resulting from the Bosch process for 3D trench fabrication reveals a densified deposit on exposed sidewall surfaces but no deposit at all on shadowed surfaces.

Finally, the very same TSD process was carried out to illustrate the shadowing effect in the 3D trench. For this purpose, the 3D trenched substrate with Aspect Ratio (AR) = 5.4 was tilted at 20° angle on the chuck [Fig. 8(a)], before a ≈ 100 nm Ta_2O_5 thin film was deposited at $V_{DC} = -140$ V. Electrical contact between the substrate and the chuck was secured by a dedicated aluminum holder. Figure 8(a) presents the expected TSD fabrication outcome, where the densified deposit is kept only on surfaces exposed to ion bombardment, after etching in diluted HF. Such exotic TSD could be of interest in future advanced nanoelectronic devices.[5,36] Figures 8(b)–8(d) show that this expectation is successfully fulfilled: a thin film is observed on the top horizontal surface of the 3D trench. When going in the depth of the trench, the film gradually transforms into Ta_2O_5 grains on sidewalls all the way down to the point where the shadowing effect prevails. Neither vertical nor horizontal deposit beyond this point of the 3D trench is observed [Figs. 8(c)–8(f), respectively]. This proof-of-concept opens up new possibilities for deposition reactor or substrate stage design, similar to concepts already used in ion beam milling machines.

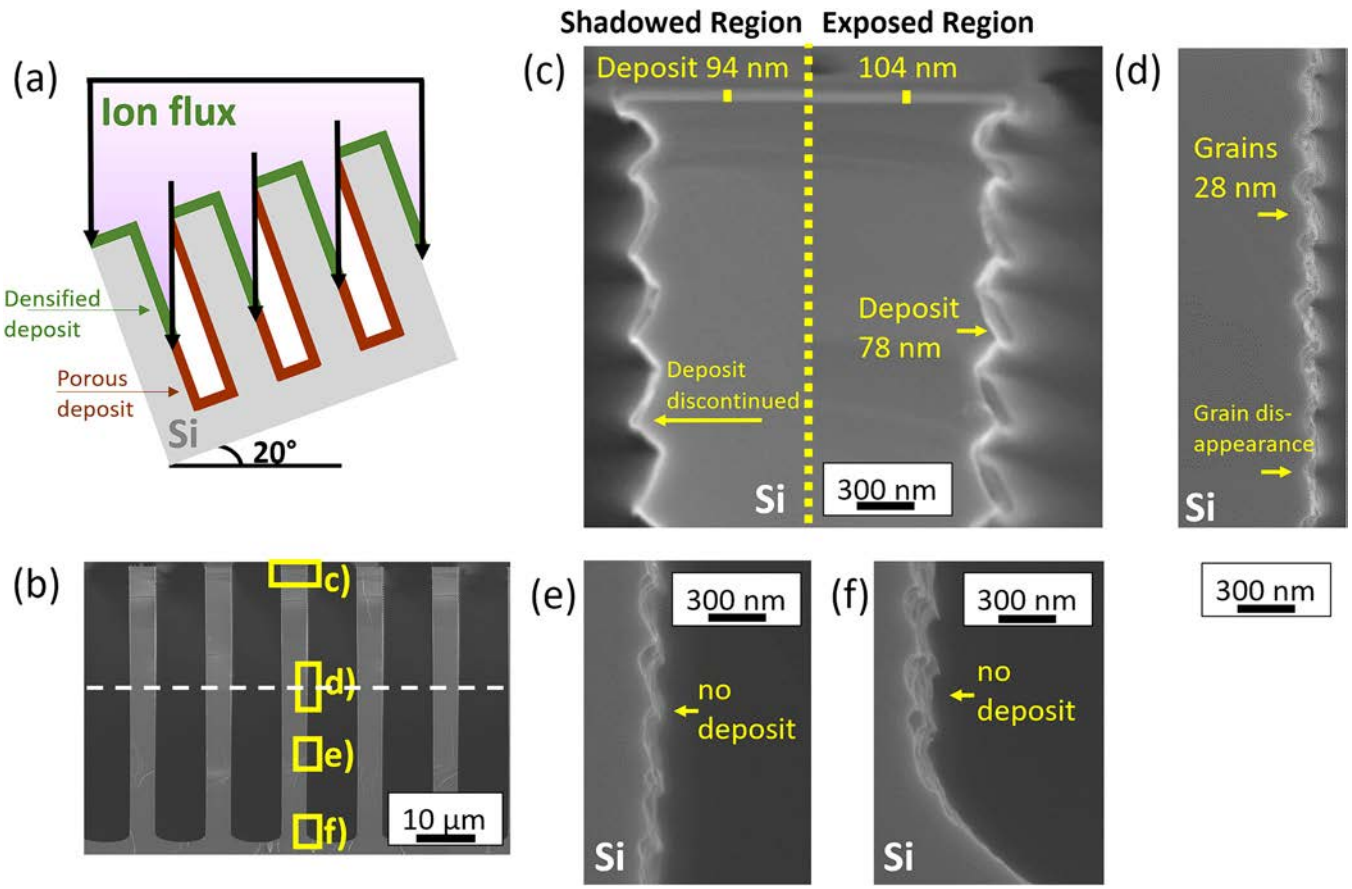

FIG. 8. (a) Schematic of the impact of ion flux on deposits in tilted and biased 3D substrates during PEALD. (b) Scanning electron microscope image of 3D trenches with AR = 5.4 and detailed images after postgrowth wet etching in 5% HF from different regions: (c) top, (d) sidewall, (e) bottom sidewall, and (f) bottom of 3D trench.

C. Outlook for selective deposition processes by combining out-of-ALD-window deposition and ion bombardment

As shown in the proof-of-concept on 3D substrates, a low processing temperature (probably below the ALD plateau) can be compensated by the extra energy provided by an ionic bombardment, whereby phenomena such as surface activation, diffusion, sputtering, and/or implantation can be enhanced. In an ICP PEALD reactor configuration, the energetic ion flux is anisotropic and is driven by the electric field across the plasma sheath so that it only affects horizontal top and bottom surfaces of 3D structures. Because of this inherent anisotropy and encouraged by the results presented in this paper, several strategies for TSD fabrication can be envisaged outside the ALD temperature plateau (hence the name out-of-ALD-window TSD) and are illustrated in Figs. 9–12. The explanation of ALD growth regime shown in Fig. 1 in Sec. I is the basis of the following reasoning.

1. First TSD strategy: Top and bottom deposition with a postdeposition etching step

As illustrated in Fig. 9, two configurations are considered starting points: (i) deposition in regime A with a low GPC, at a temperature below the ALD window [Fig. 9(a)], and (ii) deposition in regime C with a high GPC, at a temperature beyond the ALD temperature window. In the first case, ion bombardment induces an increase in the GPC thanks to the additional energy provided to the surface and shifts the growth mode from the incomplete reaction regime A to the ALD plateau regime. In the second case, the process is shifted by ionic bombardment from the ALD plateau regime to the decomposition regime C at much lower temperatures [Fig. 9(b)].

Consequently, the deposited thickness in 3D structures should be larger on horizontal surfaces than on vertical sidewalls. Thus, a dry or wet etching step (not necessarily selective) can be used to completely remove the material thickness on vertical sidewalls,

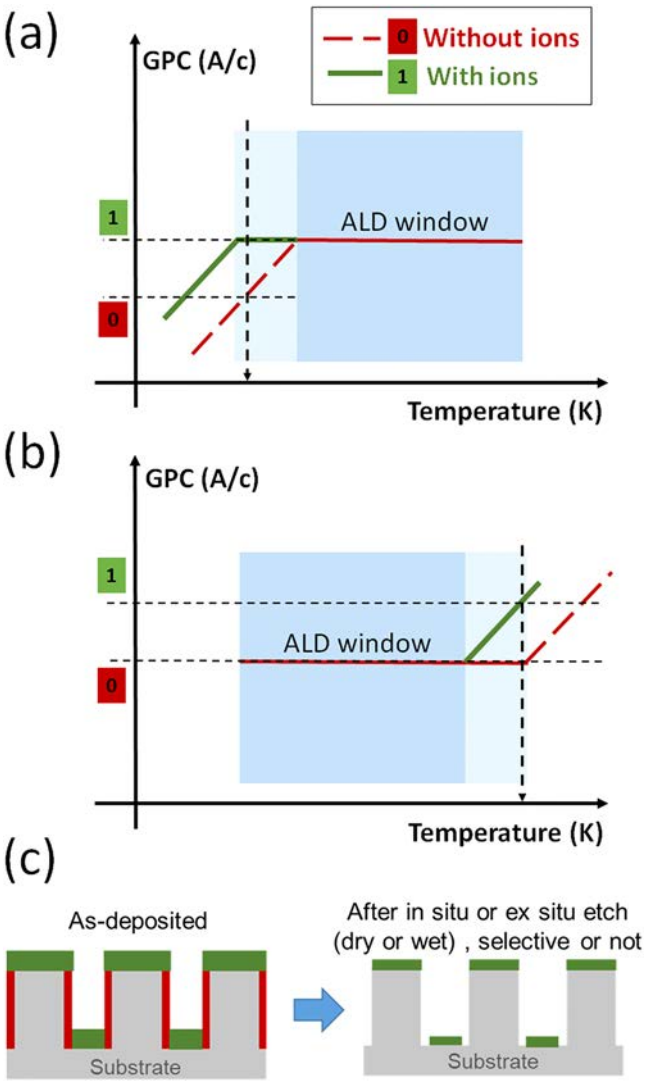

FIG. 9. Schematic illustrating the impact of ion bombardment for processes carried outside the ALD temperature window: (a) regime A: incomplete reaction; (b) regime C: precursor decomposition. (c) Schematic of horizontal TSD strategy with a postdeposition etching step.

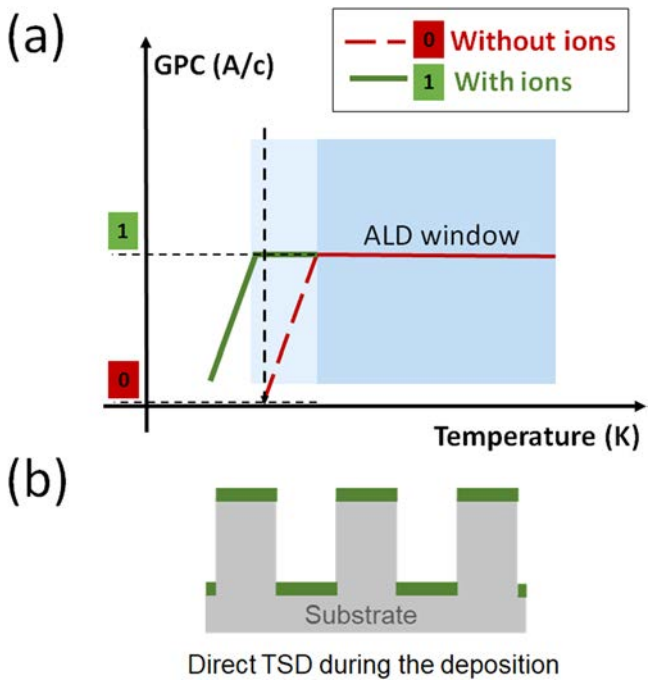

FIG. 10. (a) Schematic illustrating the impact of ion bombardment in a process carried out in regime A: incomplete reaction. (b) The resulting direct TSD strategy in 3D structures.

while simultaneously maintaining a film only on horizontal surfaces [Fig. 9(c)].

2. Second TSD strategy: Top and bottom deposition without any additional etching step

In the most incomplete reaction regime, no film growth is observed if no precursor chemisorbs or physisorbs on the substrate surface. In this case, ion bombardment assistance can initiate thin film growth only on exposed horizontal surfaces,[37] and a direct TSD without any additional postgrowth etching step can be readily achieved [Fig. 10(b)].

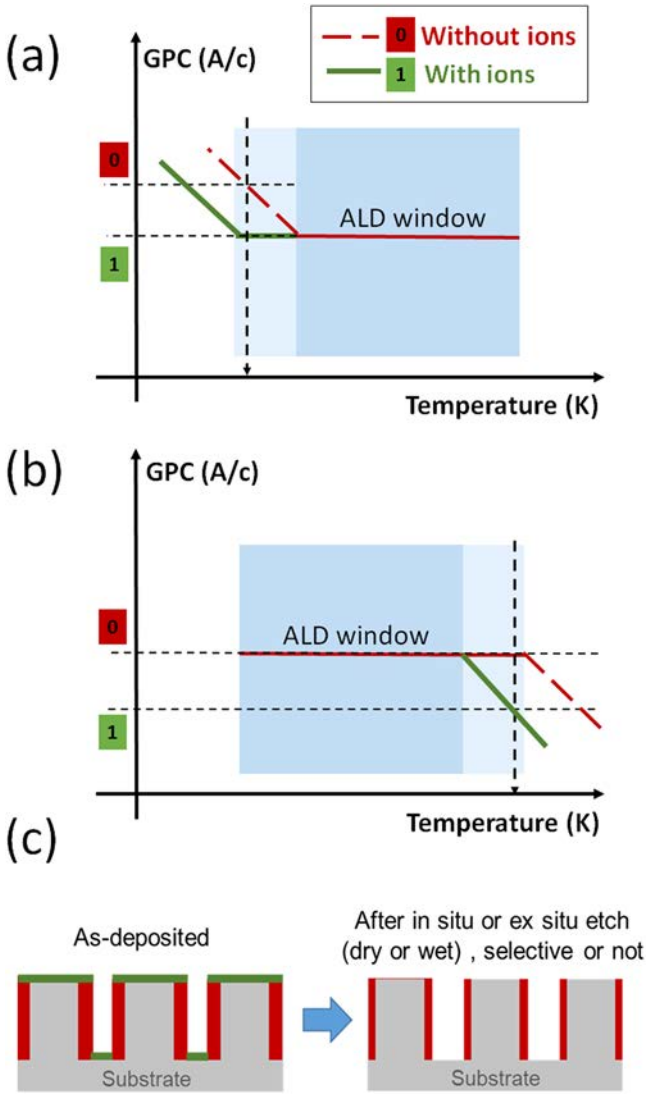

FIG. 11. Schematic illustrating the impact of ion bombardment for the process carried out outside the ALD window: (a) regime B: condensation; (b) regime D: desorption. (c) Schematic of vertical TSD strategy with a postdeposition etching step.

3. Third TSD strategy: Sidewall deposition with an additional etching step

As illustrated in Fig. 11, two new configurations are now considered starting points: (i) deposition in regime B with a large GPC at a temperature below the ALD window [Fig. 11(a)] and (ii) deposition in regime D a low GPC at a temperature above the ALD temperature window [Fig. 11(b)]. In the first case, ion bombardment during the process gives a GPC decrease thanks to the additional surface energy input and expands the lower end of the ALD temperature window to lower temperatures. In the second case, ion bombardment during the process shifts the growth regime from the ALD regime to the desorption regime D.

Subsequently, the deposited thickness in 3D structures is larger on vertical surfaces than on horizontal ones exposed to ion bombardment. Thus, a dry or wet etching step (not necessarily selective) can be used to completely remove the material thickness on horizontal surfaces, while simultaneously maintaining a film only on vertical sidewalls [Fig. 11(c)].

4. Fourth TSD strategy: Vertical deposition without any additional etching step

Like the second strategy, a process at the limit of the desorption regime D assisted by ion bombardment can lead to a direct selective deposition on vertical surfaces without any additional postdeposition etching step (Fig. 12).

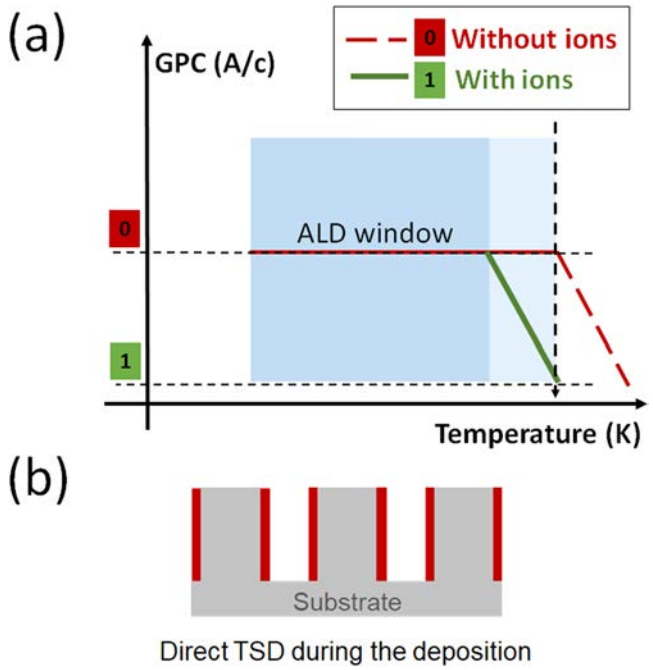

FIG. 12. (a) Schematic illustrating the impact of ion bombardment on the process carried out in regime D: desorption. (b) Subsequent direct TSD strategy in 3D structures.

To sum up on the impact of ion bombardment during the PEALD growth, it is clear that exposure to an energetic ion flux during thin film growth can contribute to locally modify the thin film GPC and density independent of the selected ALD window regime. This specific ion bombardment property provides a route toward TSD in pillared or trenched 3D patterns since thin film materials can be deposited with physical properties depending on substrate orientation with respect to the incident ion bombardment flux. To complete this TSD route, a postdeposition wet etching step carried out in diluted HF can be necessary to either selectively remove the least dense thin film material or to nonselectively remove the thinnest coating on dedicated surfaces, leaving some of the thickest deposit on surfaces of different orientations.

IV. SUMMARY AND CONCLUSIONS

In this work, we have shown that ion bombardment assistance during PEALD can enlarge the growth regime (alike ALD window plateau) to lower temperature values and can lead to significant improvements of material properties. Based on this observation, we have developed a successful TSD process with coating only on the top and bottom surfaces of 3D trenches. This TSD process consists in a standard PEALD process combined with a medium energy substrate bias applied during the plasma step. The PEALD process is then followed by a subsequent wet etching step in diluted hydrofluoric acid. This successful TSD process relies on the anisotropic character of an ion bombardment step, which increases the thin film density only on top and bottom horizontal 3D trenched surfaces, while vertical sidewalls unexposed to the ion flux are coated with a poor density material, due to processing temperatures beyond the ALD temperature window. A proof-of-concept for such a TSD process route has been provided for Ta_2O_5 thin films. This concept can most likely be extended to various precursor chemistries for oxide or nitride selective deposition by PEALD. This TSD strategy opens up new pathways for innovative TSD elaboration on temperature-sensitive substrates with high AR 3D features.

ACKNOWLEDGMENTS

The authors would like to acknowledge financial contribution from the European Union in scope of the WAKeMeUP project (No. 783176).

DATA AVAILABILITY

The data that support the findings of this study are available from the corresponding author upon reasonable request.

REFERENCES

[1]J. Liu, H. Zhu, and M. H. A. Shiraz, Front. Energy Res. **6**, 1–5 (2018).
[2]M. R. Saleem, R. Ali, M. B. Khan, S. Honkanen, and J. Turunen, Front. Mater. **1**, 18 (2014).
[3]A. J. M. Mackus, M. J. M. Merkx, and W. M. M. Kessels, Chem. Mater. **31**, 2 (2019).
[4]R. Clark, K. Tapily, K.-H. Yu, T. Hakamata, S. Consiglio, D. O'Meara, C. Wajda, J. Smith, and G. Leusink, APL Mater. **6**, 058203 (2018).
[5]G. N. Parsons and R. D. Clark, Chem. Mater. **32**, 4920 (2020).
[6]H. C. M. Knoops, T. Faraz, K. Arts, and W. M. M. Erwin Kessels, J. Vac. Sci. Technol. A **37**, 030902 (2019).
[7]D. C. Bien, H. W. Lee, and S. A. M. Badaruddin, Nanoscale Res. Lett. **7**, 288 (2012).
[8]T. Faraz *et al.*, ACS Appl. Mater. Interfaces **10**, 13158 (2018).
[9]A. Chaker, C. Vallee, V. Pesce, S. Belahcen, R. Vallat, R. Gassilloud, N. Posseme, M. Bonvalot, and A. Bsiesy, Appl. Phys. Lett. **114**, 043101 (2019).
[10]E. Stevens, Y. Tomczak, B. T. Chan, E. Altamirano Sanchez, G. N. Parsons, and A. Delabie, Chem. Mater. **30**, 3223 (2018).
[11]G. N. Parsons, J. Vac. Sci. Technol. A **37**, 020911 (2019).
[12]W.-H. Kim *et al.*, ACS Nano **10**, 4451 (2016).
[13]W. Dong, K. Zhang, Y. Zhang, T. Wei, Y. Sun, X. Chen, and N. Dai, Sci. Rep. **4**, 4458 (2014).
[14]S. D. Sherpa and A. Ranjan, J. Vac. Sci. Technol. A **35**, 01A102 (2016).
[15]R. A. Ovanesyan, E. A. Filatova, S. D. Elliott, D. M. Hausmann, D. C. Smith, and S. Agarwal, J. Vac. Sci. Technol. A **37**, 060904 (2019).
[16]C. Vallée *et al.*, J. Vac. Sci. Technol. A **38**, 033007 (2020).
[17]S. M. George, Chem. Rev. **110**, 111 (2010).
[18]T. Suntola, Mater. Sci. Rep. **4**, 261 (1989).
[19]R. L. Puurunen, J. Appl. Phys. **97**, 121301 (2005).
[20]A. J. M. Mackus, C. MacIsaac, W.-H. Kim, and S. F. Bent, J. Chem. Phys. **146**, 052802 (2016).
[21]M.-J. Choi *et al.*, Appl. Surf. Sci. **320**, 188 (2014).
[22]M. E. Dufond *et al.*, Chem. Mater. **32**, 1393 (2020).
[23]S. J. Song *et al.*, ACS Appl. Mater. Interfaces **9**(1), 537–547 (2017).
[24]S. E. Potts, W. Keuning, E. Langereis, G. Dingemans, M. C. M. van de Sanden, and W. M. M. Kessels, J. Electrochem. Soc. **157**, P66 (2010).
[25]T. Henke, M. Knaut, M. Geidel, F. Winkler, M. Albert, and J. W. Bartha, Thin Solid Films **627**, 94 (2017).
[26]V. Miikkulainen, M. Leskelä, M. Ritala, and R. L. Puurunen, J. Appl. Phys. **113**, 021301 (2013).
[27]S. E. Potts and W. M. M. Kessels, Coord. Chem. Rev. **257**, 3254 (2013).
[28]V. Beladiya *et al.*, Nanoscale **12**, 2089 (2020).
[29]T. Faraz, K. Arts, S. Karwal, H. C. M. Knoops, and W. M. M. Kessels, Plasma Sources Sci. Technol. **28**, 024002 (2019).
[30]N. E. Richey, C. de Paula, and S. F. Bent, J. Chem. Phys. **152**, 040902 (2020).
[31]W. J. Maeng and H. Kim, Electrochem. Solid State Lett. **9**, G191 (2006).
[32]T. Blanquart, V. Longo, J. Niinistö, M. Heikkilä, K. Kukli, M. Ritala, and M. Leskelä, Semicond. Sci. Technol. **27**, 074003 (2012).
[33]A. J. M. Mackus, A. A. Bol, and W. M. M. Kessels, Nanoscale **6**, 10941 (2014).
[34]S. B. S. Heil, F. Roozeboom, M. C. M. van de Sanden, and W. M. M. Kessels, J. Vac. Sci. Technol. A **26**, 472 (2008).
[35]Y. Tomczak, K. Knapas, M. Sundberg, M. Leskelä, and M. Ritala, Chem. Mater. **24**, 1555 (2012).
[36]T. E. Seidel and M. I. Current, J. Vac. Sci. Technol. A **38**, 022602 (2020).
[37]S.-S. Lim, I.-H. Baek, K.-C. Kim, S.-H. Baek, H.-H. Park, J.-S. Kim, and S. K. Kim, Ceram. Int. **45**, 20600 (2019).